ALTERNATING ANGLE MINIMIZATION BASED UNMIXING WITH ENDMEMBER VARIABILITY

Rob Heylen[*]*, Paul Scheunders*[*]*, Alina Zare*[†]*, Paul Gader*[‡]

[*]IMinds-Visionlab, University of Antwerp, Belgium
[†] Electrical and computer engineering, University of Missouri, USA
[‡] Computer and information science and engineering, University of Florida, USA

ABSTRACT

Several techniques exist for dealing with spectral variability in hyperspectral unmixing, such as multiple endmember spectral mixture analysis (MESMA) or compositional models. These algorithms are computationally very involved, and often cannot be executed on problems of reasonable size. In this work, we present a new algorithm for solving the unmixing problem when spectral variability is present. The algorithm uses a library-based approach to describe the variability present in each class, and executes an alternating optimization with respect to these libraries. The optimization problem itself is constructed as an angle minimization problem by exploiting the geometrical interpretation of the unmixing problem. This results in an algorithm which yields almost identical results as MESMA, but is computationally much more favorable.

Index Terms— Spectral unmixing, hyperspectral image processing

1. INTRODUCTION

In many spectral unmixing approaches, one assumes that a single endmember spectrum is available to represent each pure material present in the scene. This assumption is often not realistic in practice, as several materials show some inherent variability due to subtle differences in makeup, orientation, or composition. For instance, a scene can contain many pixels which could be considered pure vegetation or soil, but the corresponding spectra will show small differences.

Two general approaches exist to describe and deal with spectral variability: distribution or library based. In distribution-based approaches one describes spectral variability by modeling it as a probability distribution. Examples are the normal compositional model (NCM) or the beta compositional model (BCM). Alternatively, one can build a large library of representative spectra from each class, and use an algorithm which selects the best subset of library spectra to unmix each target spectrum. The best known example of the latter approach is the MESMA algorithm [1]. Both the distribution and library-based approaches are computationally very demanding when the problem sizes become relatively large, as the former approach employs Bayesian inference, and the latter tries to solve a combinatorial optimization problem.

In this work, we propose an alternative for the MESMA algorithm, which aims to solve the same optimization problem, but without resorting to a classical brute-force approach. The proposed alternating angle minimization (AAM) algorithm is based on an alternating optimization approach, where one iteratively finds the best candidate endmember in each library until convergence has been reached. By writing this optimization problem as an angle minimization problem, a very high computational efficiency can be reached, while the obtained results are very similar to those obtained with a brute-force MESMA approach.

2. THE MESMA ALGORITHM

The MESMA algorithm is based on the linear mixing model (LMM), where a pixel $\boldsymbol{x}$ can be expressed as a linear combination of endmember spectra subject to an abundance sum-to-one constraint (ASC) and an abundance non-negativity constraint (ANC):

$$\boldsymbol{x} = \sum_{i=1}^{p} a_i \boldsymbol{e}_i + \boldsymbol{\eta}, \qquad \begin{cases} \forall i : a_i \geq 0 & \text{(ANC)} \\ \sum_i a_i = 1 & \text{(ASC)} \end{cases} \tag{1}$$

To capture spectral variability, spectral libraries are available for each class. Consider p endmember libraries $\{L_1, \ldots, L_p\}$, where library L_i has N_i elements. MESMA then tries to identify the subset of endmembers, one from each library, which generates the smallest reconstruction error (RE), defined as the Euclidean distance between the target spectrum and the spectrum reconstructed under the LMM. In practice, if no early stopping rules are implemented, this process involves unmixing each target spectrum with respect to every possible endmember combination, resulting in $\prod_i N_i$ fully-constrained least-squares unmixing (FCLSU) operations.

As FCLSU is a computationally expensive operation, an alternative approach based on sum-to-one constrained least-

squares unmixing (SCLSU) can be employed as well. The idea is to perform SCLSU with respect to every subset of libraries as well, and retain only solutions which respect the ANC. This requires $\prod_i (N_i + 1)$ SCLSU operations, and yields the same result as the FCLSU approach. As SCLSU is computationally much cheaper than FCLSU, this latter approach is typically faster.

3. ALTERNATING ANGLE MINIMIZATION

We propose an alternating optimization technique for solving the same minimization problem as the MESMA algorithm tries to solve, i.e., finding the subset of endmembers with the smallest RE, where each endmembers has to be selected from a corresponding library. The optimization aims to find the best endmember from each library in turn, until convergence has been reached. While the global optimization problem is a combinatorial problem and very hard to solve, the optimization with respect to a single library can be done very efficiently by exploiting the geometrical interpretation of the unmixing problem.

As described in several papers [2, 3], solving the SCLSU problem is equivalent to projecting the target $\boldsymbol{x}$ orthogonally onto the hyperplane $H(E)$ through the endmembers in E. The RE is then given by the distance from $\boldsymbol{x}$ to this projection: $\|\boldsymbol{x} - P_{H(E)}(\boldsymbol{x})\|$. If we define $F = E/\{\boldsymbol{e}_p\} = (\boldsymbol{e}_1, \ldots, \boldsymbol{e}_{p-1})$, using standard geometrical relations one can write this distance as

$$\left\|\boldsymbol{x} - P_{H(E)}(\boldsymbol{x})\right\| \quad = \quad \left\|\boldsymbol{x} - P_{H(F)}(\boldsymbol{x})\right\| \sin(\theta) \qquad (2)$$

with

$$\begin{aligned} \theta &= \min(\alpha, \pi - \alpha) \\ \alpha &= \sin^{-1}\left(\frac{\left\|\boldsymbol{x} - P_{H(E)}(\boldsymbol{x})\right\|}{\left\|\boldsymbol{x} - P_{H(F)}(\boldsymbol{x})\right\|}\right) \end{aligned} \qquad (3)$$

This is illustrated for a three-endmember scenario in Fig. 1. Remark that the roles of $\boldsymbol{x}$ and $\boldsymbol{e}_p$ can also be interchanged: With $G = F \cup \boldsymbol{x} = (\boldsymbol{e}_1, \ldots, \boldsymbol{e}_{p-1}, \boldsymbol{x})$, we have

$$\alpha \quad = \quad \sin^{-1}\left(\frac{\left\|\boldsymbol{e}_p - P_{H(F)}(\boldsymbol{e}_p)\right\|}{\left\|\boldsymbol{e}_p - P_{H(G)}(\boldsymbol{e}_p)\right\|}\right) \qquad (4)$$

This observation can be used to rewrite the single-library optimization problem as an angle minimization. Consider $p-1$ fixed endmembers in $F = (\boldsymbol{e}_1, \ldots, \boldsymbol{e}_{p-1})$, and a final endmember $\boldsymbol{e}_p$ which can be chosen from a library L_p with N_p elements. Because $\left\|\boldsymbol{x} - P_{H(F)}(\boldsymbol{x})\right\|$ is constant, (2) states that the endmember with the smallest angle θ will also minimize the RE.

This optimization can be carried out for each library in turn, which will decrease the RE at each step until a final set of endmembers is reached. While this is not guaranteed to be a global minimum, we expect this to be a good candidate solution for this minimum. This is also confirmed by our experimental results.

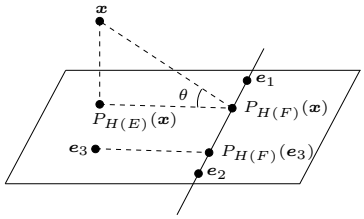

Fig. 1: Illustration of relation (2).

Because this technique is based on the geometrical interpretation of the SCLSU problem, we employ a similar strategy as in the MESMA algorithm to obtain FCLSU results: We consider all possible subsets of libraries and perform the iterative optimization for each subset. The solution with the smallest RE is returned after considering all subsets. The AAM algorithm is given in Algorithm 1.

Algorithm 1: AAM algorithm

```
Select a number of iterations K.
for Every non-empty subset S ⊂ {1,...,p} do
    Let q = |S| be the cardinality of S
    Let e_j^i be shorthand for L_{S_i}(j), endmember j from library L_{S_i}
    Select a random index set {I_i}_{i=1}^q, I_i ∈ 1,...,N_{S(i)}.
    for iteration ∈ [1,...,K] do
        for i ∈ [1,...,q] do
            F = {e_{I_1}^1, ..., e_{I(i-1)}^{i-1}, e_{I(i+1)}^{i+1}, ..., e_{I_q}^q}
            G = F ∪ x
            for n ∈ [1,...,N_{S(i)}] do
                p_n = sin^{-1}( ||e_n^i − P_{H(F)}(e_n^i)|| / ||e_n^i − P_{H(G)}(e_n^i)|| )
                if (x − P_{H(F)}(x))·(e_n^i − P_{H(F)}(e_n)) < 0 then
                    p_n = π − p_n
            I_i = argmin_n({p_n}_{n=1}^{N_i})
    E = {e_{I_1}^1, ..., e_{I_q}^q}
    a(S) = FCLSU(x, E)
    RE(S) = ||x − Ea(S)||
Return results corresponding with min(RE)
```

While the computational complexity of the MESMA algorithm scales as $\prod_i N_i$ with the library sizes, the AAM algorithm scales linearly in the sizes of the libraries. This suggests that the AAM algorithm will be much faster than MESMA

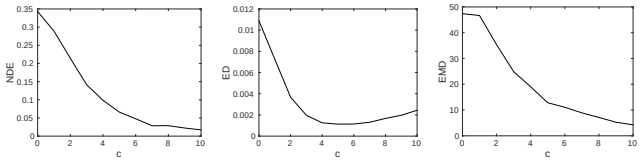

(a) NDE (b) ED (c) EMD

Fig. 2: The NDE between the endmember sets, the ED between the abundance vectors, and the pixel-wise EMD as defined in [4], averaged over 100 random instances with 100 pixels each, with a given value of c.

and other alternative algorithms in many practical scenarios, and can treat situations which become computationally intractable with the alternatives.

4. RESULTS

4.1. Artificial data sets

Several properties of the AAM algorithm can be tested and demonstrated on artificial data sets. The data set consists of points in a $d = 200$ dimensional space. Each library is created as a d-dimensional random unit Gaussian distribution, centered around the point k_i. These centers $\{k_i\}_{i=1}^{p}$ are randomly selected from a Gaussian distribution with standard deviation c. The data set $\{\boldsymbol{x}_i\}_{i=1}^{N}$ itself is selected from a unit Gaussian distribution around the origin. This way, the libraries and the data will show large overlaps (or correlation) for low values of c, and will be more independent for larger values of c. For simplicity, each library contained the same number of spectra.

We employ three different measures to assess unmixing results with variability: The number of different endmembers (NDE) selected from each library, the Euclidean distance (ED) between the abundance vectors, and the Earth mover's distance (EMD) as proposed in [4]. The latter metric allows the comparison of unmixing results taking differences in both endmembers and abundances into account. Fig. 2 shows these measures as a function of c, averaged over 100 random instances of 100 pixels with $p = 4$ libraries, each containing 10 spectra.

The runtime of MESMA and the AAM algorithm on these data sets are displayed in Fig. 3 for different parameters. This figure illustrates clearly that the computational cost rises quickly for MESMA as a function of the library sizes, but hardly increases for the AAM algorithm.

4.2. Hyperspectral images

We executed the AAM algorithm on real data sets as well, and compare the obtained results with those obtained by MESMA, and by FCLSU where the library averages were used as endmembers. The data set under consideration is also

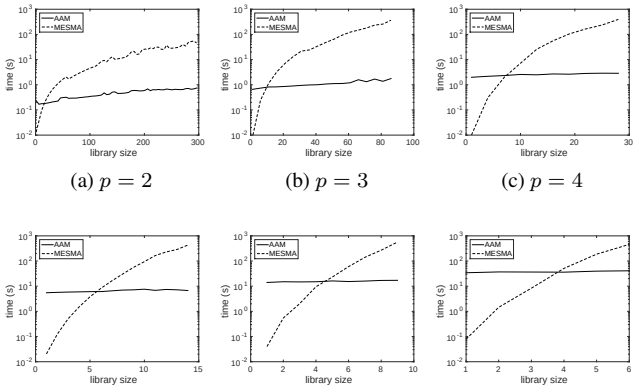

(a) $p = 2$ (b) $p = 3$ (c) $p = 4$

(d) $p = 5$ (e) $p = 6$ (f) $p = 7$

Fig. 3: The runtime in seconds of the AAM algorithm and MESMA as a function of library size, for different values of the number of libraries p. All libraries are equally sized.

used in [5] to assess the BCM, and was collected in Longbeach, Missouri, USA. This 13×19 pixel subset contains four classes of materials, i.e. an asphalt road, yellow curb, grass and oak trees. Spectral libraries were collected in the field using a hand-held spectrometer, with 10 spectra for the asphalt class, 10 for yellow curb, 50 for grass and 10 for the oak leaves. Both the image and the endmember libraries contain 53 spectral bands.

The unmixing results obtained by these methods are shown in Fig. 4, where each row corresponds with a class and each column with an unmixing technique or the ground truth. It can be observed that the AAM and the MESMA method both yield very similar results, and only differ in a handful of pixels.

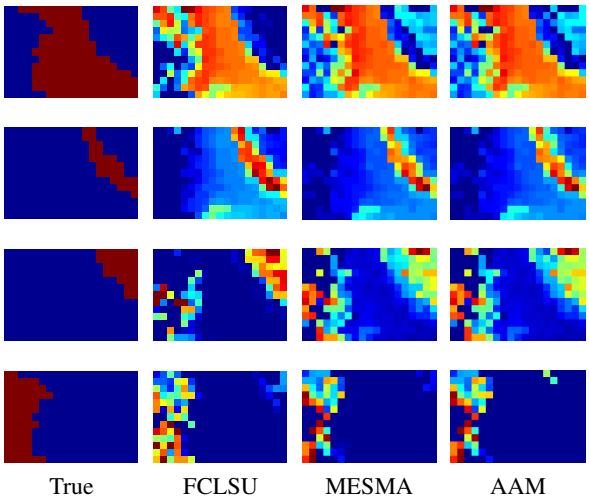

True FCLSU MESMA AAM

Fig. 4: Long-beach abundance maps. Top to bottom: Alphalt, yellow curb, grass, oak leaves

The differences between the results obtained by MESMA and the AAM algorithm are illustrated in Fig. 5, where the NDE, the ED and the EMD between the unmixing results are shown as color maps. It is clear that identical endmembers and abundances are obtained for most pixels, and that possible deviations typically stay small. Furthermore, one or two misidentified endmembers do not always automatically lead to large abundance errors. The endmembers obtained with the AAM algorithm can be very similar to those obtained with MESMA, or the corresponding abundance can be small. Both situations would lead to small abundance errors, even with misidentified endmembers.

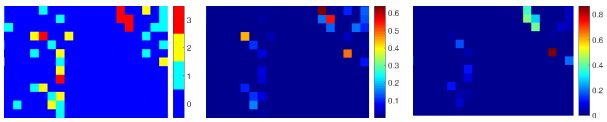

(a) NDE (b) ED (c) EMD

Fig. 5: Illustration of the differences between the MESMA and the AAM algorithm: The number of different endmembers (a), the ED between the abundance vectors (b) and the EMD between the unmixing results (c).

Processing this data set took 0.17s for the FCLSU algorithm, 16s for MESMA, and 6s for the AAM algorithm. Remark that the employed libraries are relatively small, and that the runtime required for MESMA will increase significantly for larger libraries.

5. DISCUSSION

We have introduced a new technique for solving unmixing problems which include spectral variability represented through spectral libraries. This AAM algorithm is based upon iterative optimization with respect to each library in turn. We demonstrated the algorithm on artificial data sets, and on a small real hyperspectral image. These results indicate that for most pixels, identical results as MESMA are obtained, and that possible deviations typically stay small. The proposed algorithm has a much more favorable scaling with the problem size, as the computational requirements scale linearly in the library sizes. This allows the technique to be executed on larger problems as well.

In the near future we intend to assess the AAM algorithm on larger hyperspectral data sets, and to run more detailed comparisons with alternative unmixing methods such as the compositional models.

6. REFERENCES

[1] D.A. Roberts, M. Gardner, R. Church, S. Ustin, G. Scheer, and R.O. Green, "Mapping chaparral in the santa monica mountains using multiple endmember spectral mixture models," *Remote Sens. Environ.*, vol. 65, pp. 267–279, 1998.

[2] P. Bajorski, "Simplex projection methods for selection of endmembers in hyperspectral imagery," *Proc. IEEE IGARSS*, vol. 5, pp. 3207–3210, 2004.

[3] R. Heylen and P. Scheunders, "Fully constrained least-squares spectral unmixing by simplex projection," *IEEE Trans. Geosci. Remote Sens.: Spec. iss. Remote Sensing*, vol. 49, no. 11, pp. 4112–4122, 2011.

[4] A. Zare and D. Anderson, "Earth movers distance-based simultaneous comparison of hyperspectral endmembers and proportions," *IEEE J. Sel. Top. Appl. Earth Obs. Remote Sens.*, vol. 7, no. 6, pp. 1910–1921, June 2014.

[5] X. Du, A. Zare, P. Gader, and D. Dranishnikov, "Spatial and spectral unmixing using the beta compositional model," *IEEE J. Sel. Top. Appl. Earth Obs. Remote Sens.*, vol. 7, no. 6, pp. 1994–2003, June 2014.